Biology of Reproduction, 2022, **106(6)**, 1083–1097
https://doi.org/10.1093/biolre/ioac029
Advance access publication date 3 February 2022
Research Article

Chemokine C-X-C receptor 4 mediates recruitment of bone marrow-derived nonhematopoietic and immune cells to the pregnant uterus†

Yuan-Yuan Fang, Fang Lyu, Nafeesa Abuwala, Aya Tal, Alice Y. Chen, Hugh S. Taylor and Reshef Tal*

Department of Obstetrics, Gynecology and Reproductive Sciences, Yale School of Medicine, New Haven, CT, USA

***Correspondence:** Department of Obstetrics, Gynecology and Reproductive Sciences, Yale School of Medicine, New Haven, CT 06510, USA. Tel: +1-203-785-4005; Fax: +1-203-785-7819; E-mail: reshef.tal@yale.edu

†**Grant Support:** This work was supported by funds from the Eunice Kennedy Shriver National Institute of Child Health and Human Development (NICHD) (grant 5K12HD047018 to HST and RT), the Robert E. Leet and Clara Guthrie Patterson Fellowship award (to RT), and the Albert S. McKern award (to RT).

Abstract

Bone marrow-derived progenitor cells (BMDPCs) are mobilized to the circulation in pregnancy and get recruited to the pregnant decidua where they contribute functionally to decidualization and successful implantation. However, the molecular mechanisms underlying BMDPCs recruitment to the decidua are unknown. CXCL12 ligand and its CXCR4 receptor play crucial roles in the mobilization and homing of stem/progenitor cells to various tissues. To investigate the role of CXCL12–CXCR4 axis in BMDPCs recruitment to decidua, we created transgenic GFP mice harboring CXCR4 gene susceptible to tamoxifen-inducible Cre-mediated ablation. These mice served as BM donors into wild-type C57BL/6 J female recipients using a 5-fluorouracil-based nongonadotoxic submyeloablation to achieve BM-specific CXCR4 knockout (CXCR4KO). Successful CXCR4 ablation was confirmed by RT-PCR and in vitro cell migration assays. Flow cytometry and immunohistochemistry showed a significant increase in GFP+ BM-derived cells (BMDCs) in the implantation site as compared to the nonpregnant uterus of control (2.7-fold) and CXCR4KO (1.8-fold) mice. This increase was uterus-specific and was not observed in other organs. This pregnancy-induced increase occurred in both hematopoietic (CD45+) and nonhematopoietic (CD45–) uterine BMDCs in control mice. In contrast, in CXCR4KO mice there was no increase in nonhematopoietic BMDCs in the pregnant uterus. Moreover, decidual recruitment of myeloid cells but not NK cells was diminished by BM CXCR4 deletion. Immunofluorescence showed the presence of nonhematopoietic GFP+ cells that were negative for CD45 (panleukocyte) and DBA (NK) markers in control but not CXCR4KO decidua. In conclusion, we report that CXCR4 expression in nonhematopoietic BMDPCs is essential for their recruitment to the pregnant decidua.

Summary statement: Expression of CXCR4 receptor in nonhematopoietic bone marrow-derived progenitor cells is essential for their recruitment to the decidua during pregnancy.

Received: November 16, 2021. **Revised:** January 24, 2022. **Accepted:** January 28, 2022

Graphical Abstract

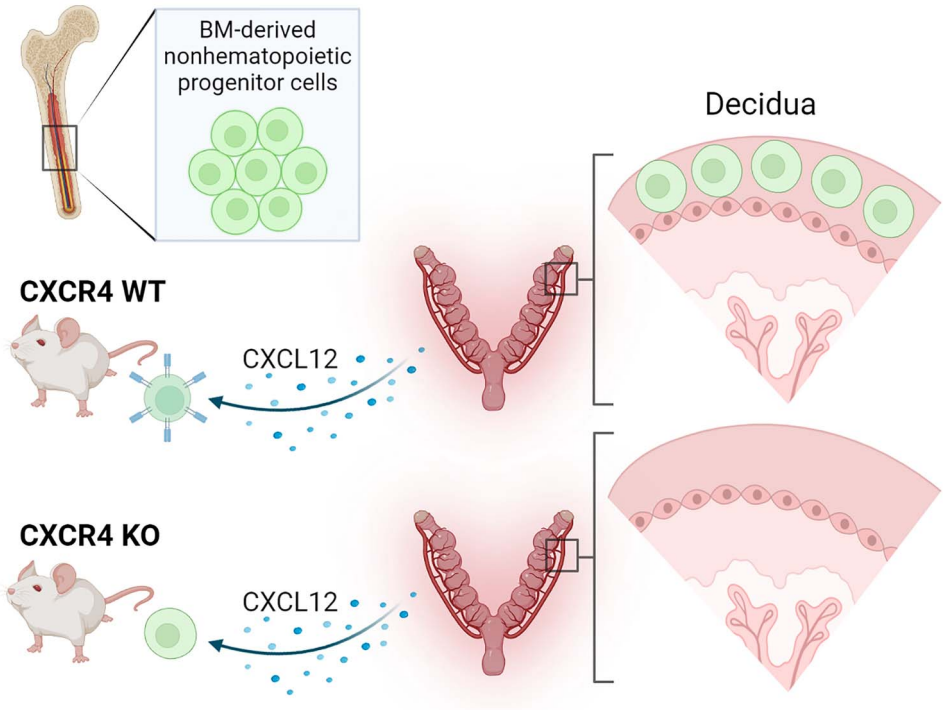

Keywords: bone marrow, CXCR4, implantation, pregnancy, stem cells, uterus

Introduction

The G-protein coupled chemokine receptor C-X-C chemokine receptor type 4 (CXCR4) belongs to the cysteine-X-cysteine (C-X-C) family, which is involved in various biological processes including leukocyte adhesion and transendothelial migration, cellular proliferation, differentiation, apoptosis, angiogenesis, and immune regulation [1]. The interaction between CXCR4 and its cognate C-X-C motif chemokine ligand 12 (CXCL12), also known as stromal derived factor 1 (SDF-1), plays an important role in regulating the bone marrow (BM) retention of hematopoietic stem and progenitor cells, their maintenance and subsequent mobilization from the BM niche [2–5]. CXCR4 is expressed in a variety of tissues and cell types, including B cells, T-lymphocytes, monocytes, neutrophils, endothelial cells, epithelial cells, and stromal cells [6]. Global ablation of CXCL12 or CXCR4 is embryonic lethal with abnormalities in bone and marrow formation, the immune system, and cardiovascular development [7, 8].

The CXCR4 receptor is expressed on the surface of stem cells and is functionally important for stem cell migration [9]. Consistent with this, it has been demonstrated that the CXCL12–CXCR4 pathway has crucial roles in the mobilization, maintenance, and homing of stem cells [10, 11]. Notably, a recent study has shown that CXCR4 expression in the bone marrow microenvironment is an important factor for hematopoietic stem and progenitor cell maintenance and regeneration [12].

The CXCL12–CXCR4 axis plays an important role at the maternal–fetal interface in humans and other mammalian species. The endometrium expresses CXCL12 and CXCR4, and expression of both genes is upregulated in the decidua during embryo implantation [13, 14]. The CXCL12 protein is expressed in endometrial epithelial cells and is also highly expressed in human endometrial stromal cells [14–16], and its production is stimulated by estradiol in a time-dependent and dose-dependent manner [15, 17]. The CXCR4 receptor protein is localized in stromal cells, vascular endothelial cells, and immune cells in the endometrium [14]. In humans, CXCL12 has been shown to mediate recruitment of CXCR4-expressing natural killer (NK) cells into the decidua [18, 19]. In mice, CXCL12 at the maternal–fetal interface increases the migration of regulatory T (Treg) cells into the uterus during pregnancy [20]. In addition, CXCL12 ligand and its CXCR4 receptor mediate migration of BM cells toward endometrial stromal cells and myometrial stomal cells in vitro [15, 21], suggesting a possible role of CXCL12 in recruiting stem cells to the uterus. Using a 5-fluorouracil (5-FU)-based nongonadotoxic bone marrow transplantation (BMT) [22], we have shown in mice that BM-derived progenitor cells (BMDPCs) are mobilized to the circulation in pregnancy, and get recruited to the pregnant decidua where they become decidual stromal cells and contribute functionally to successful embryo implantation and decidualization [23]. These BMDPCs also contribute to endothelial cells as part of decidual vasculature in a process termed vasculogenesis [24], and to epithelial, stromal, and endothelial endometrial compartments in the involuting uterus during physiological postpartum remodeling [25]. However, the molecular mechanisms responsible for the recruitment of these nonhematopoietic BMDPCs to the decidua during pregnancy are still unknown.

Our objective was to test the hypothesis that the CXCL12–CXCR4 axis mediates the recruitment of nonhematopoietic BMDPCs to the uterus during implantation. For this end, we created a nongonadotoxic BM transplant mouse model harboring specific CXCR4 knockout in adult BM cells using Cre-LoxP technology. Transgenic mice expressing Cre recombinase under the control of the tamoxifen-inducible promoter in conjunction with floxed CXCR4 genes and GFP served as BM donors into wild-type (WT) recipients to produce inducible CXCR4 ablation specifically in BM cells. Here, we report that CXCR4 expression in BMDPCs is necessary for their recruitment to the pregnant decidua.

Materials and methods

Ethics statement

Mice were maintained in a controlled environment at the Animal Facility of Yale School of Medicine with a 12-h light, 12-h dark cycle with ad libitum access to food and water. All animal procedures were performed according to an approved Yale University Institutional Animal Care and Use Committee protocol (#07113).

Animals and mice generation

To generate tamoxifen-inducible CXCR4 knockout mice, we used the Cre/LoxP tamoxifen-inducible system. All mice were purchased from Jackson Laboratories (Bar Harbor, ME). All animals had C57Bl/6 J background. Mice expressing the Cre recombinase gene under the control of the tamoxifen-inducible promoter (B6.Cg-Tg(CAG-Cre/Esr1*)5Amc/J, stock no. 004682) were bred with mice with floxed Cxcr4 alleles (B6.129P2-Cxcr4^{tm2Yzo}/J, stock no. 008767). In the CAG-Cre-Esr1 mice, the Cre recombinase is fused with a mutated ligand-binding domain (LBD) of the estrogen receptor (ER), which has a very high affinity for the synthetic ER ligand tamoxifen (TM) but lacking in sensitivity to endogenous estrogen [26, 27]. CXCR4$^{flox/flox}$ mice have the CXCR4 floxed allele, in which exon 2 (2.2 kbp) is flanked by two loxP sequences [8]. This breeding generated TM-inducible CXCR4$^{flox/flox}$ mice (iCXCR4$^{flox/flox}$), which in turn were cross-bred with transgenic mice expressing the GFP reporter gene under control of the ubiquitin C promoter (C57BL/6-Tg(UBC-GFP)30Scha/J, stock number 004353) to generate iCXCR4$^{flox/flox}$/GFP mice, enabling to track BM cells originating from these mice. Upon TM administration, TM binds to the Cre-recombinase allowing its translocation to the nucleus where it causes site-specific recombination of the LoxP sites resulting in knockout of CXCR4 gene (Figure 1A). For animal experiments, TM-inducible CXCR4$^{flox/flox}$ with GFP transgene (Cre^{+}CXCR4$^{flox/flox}$/GFP) and their Cre-negative Cxcr4$^{flox/flox}$/GFP (Cre^{-}CXCR4$^{flox/flox}$/GFP) littermates were used. After TM administration, Cre^{+}CXCR4$^{flox/flox}$/GFP will be referred to as CXCR4KO, while Cre^{-}Cxcr4$^{flox/flox}$/GFP will be referred to as WT controls. Bone marrow and peripheral blood were obtained from CXCR4KO and WT control mice to confirm knockout of CXCR4 by RT-PCR and functional assays as detailed below.

Genotyping

Total DNA was extracted from ear skin of mice using the DNeasy blood and tissue kit (Qiagen) and Direct PCR lysis reagent (Qiagen) according to the manufacturer's protocol. The genomic DNA was subjected to PCR with specific primers to determine the genotype. PCR was also performed to detect the deletion of the floxed CXCR4 gene [28] in Cre^{+}CXCR4$^{flox/flox}$ but not Cre^{-}CXCR4$^{flox/flox}$ controls following TM administration. The primers used for *CXCR4* wild-type gene were: 5′-CCACCCAGGACAGTGTGACTCTAA-3′ (forward) and 5′-GATGGGATTTCTGTATGAGGATTAGC-3′ (reverse); *CXCR4* floxed gene, 5′- CCTCGGAATGAAGAGATTATG-3′ (forward) and 5′-GTCAGAATCCTCCAGTTTTCA-3′ (reverse); TM-inducible *Cre* transgene, 5′-CGTGATCTGCA-ACTCCAGTC-3′ (forward) and 5′-AGGCAAATTTTGGTG-TACGG-3′ (reverse); *GFP* transgene, 5′-AAGTTCATCAGC-ACCACCG-3′ (forward) and 5′-TCCTTGAAGAAGATGG-TGCG-3′ (reverse). A second set of CXCR4-specific primers was used to detect deletion of the floxed allele following Cre recombination: 5′-CACTACGCATGACTCGAAATG-3′ (forward) and 5′-CCTCGGAATGAAGAGATTATG-3′.

Experimental bone marrow transplantation model

Six-week-old female C57BL/6 J WT mice received 5-FU-based nongonadotoxic BM conditioning before BMT as previously described [22, 23]. A schematic of the experimental design is shown in Figure 1B. Submyeloablation was performed by intraperitoneal injections of 125 mg/kg 5-FU on day −6 and day −1 before BMT, and three intraperitoneal injections of 50 μg/kg stem cell factor (SCF) (150 μg/kg total) at 21 and 9 h before, and 3 h after the second 5-FU dose. Bone marrow was extracted from 6 to 10-week-old Cre^{+}CXCR4$^{flox/flox/}$GFP and Cre^{-}CXCR4$^{flox/flox/}$GFP (control) donor mice as previously described [22]. Briefly, BM cells were flushed from tibias and femurs into cold sterile DMEM-F12 media, and filtered through a 70 μm filter mesh to remove any tissue clumps and bony spicules. Following filtration, the cells were washed by centrifugation and resuspended in phosphate-buffered saline (PBS) twice prior to injection. BMT was carried out by retro-orbital injection of 20×10^6 unfractionated BM cells into the WT recipient mice through the retro-orbital vein on day 0 after BM conditioning of the recipient mice as described above. Toxicity was monitored daily with weight measurements and general wellbeing assessment.

Following a 3-week recovery period, donor chimerism was assessed using flow cytometry to detect GFP+ cells in peripheral blood obtained by venipuncture. Tamoxifen was subsequently administered by IP injection to BM-engrafted mice at 75 mg/kg body weight for five consecutive days to induce BM-specific CXCR4 knockout. CXCR4 knockout in transplanted BM cells was then determined 2 weeks following the last tamoxifen dose by assaying peripheral blood for Cxcr4 mRNA expression as described below. After successful establishment of this animal model, female BMT recipients were then bred for up to 1 week with 12- to 14-week-old C57BL/6 fertile male mice (1:2 male to female ratio) and checked at 8 a.m. daily for vaginal plugs. Upon vaginal plug detection the female was separated from the male and the morning of plug detection was considered embryonic day 0.5 (E0.5). The E9.5 pregnant mice and nonpregnant virgin controls (at estrus stage) were euthanized and blood, BM, spleen, and uterine implantation sites and uterine horns (nonpregnant) were collected for flow cytometry analysis of single cells. In addition, uterine tissues were collected in 4% paraformaldehyde for histology and immunohistochemistry.

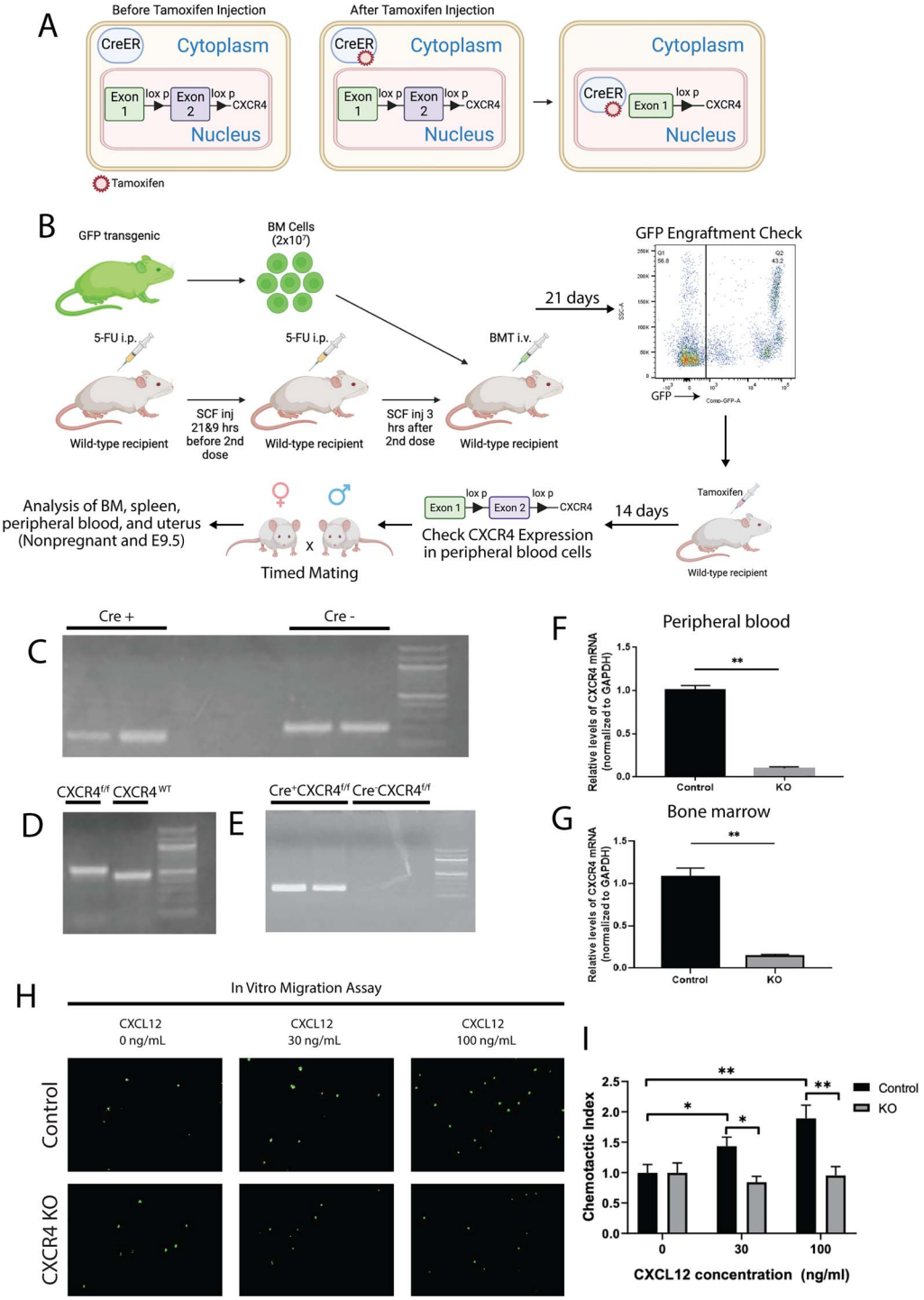

Figure 1. (A) A schematic describing the Cre-Lox system utilized in our model. In the CAG-Cre-Esr1 mice, the Cre recombinase is fused with a mutated LBD of the ER, which has very high affinity to the synthetic ER ligand tamoxifen while lacking sensitivity to endogenous estrogen. Upon tamoxifen administration, Cre recombinase translocates to the nucleus where it excises exon 2 of the CXCR4 gene flanked by the LoxP sites. (B) A schematic of the experimental model. WT C57BL/6 J recipient female mice received nongonadotoxic submyeloablative BMT regimen using 5-FU injections on day −6 and day −1 before BMT and SCF injections at −21 and −9 h prior to and +3 h after the second 5FU dose. $Cre^{+}CXCR4^{flox/flox}/GFP^{+}$ (CXCR4KO) or $Cre^{-}CXCR4^{flox/flox}/GFP^{+}$ (WT) mice served as BM donors. BM engraftment was assayed by flow cytometry of peripheral blood on day 21 post-BMT. Subsequently, engrafted female mice received intraperitoneal injection of Tamoxifen at 75 mg/kg body weight for five consecutive days. BMT recipients were mated with fertile males on day 14 post-tamoxifen injections and timed pregnancies were established. Pregnant mice were sacrificed on E9.5 or as nonpregnant (controls). Blood, BM, spleen, and uterus were collected from pregnant and nonpregnant controls and analyzed using multicolor flow cytometry, IHC, and IF. (C and D) Genotyping PCR results for detection of (C) Cre + and (D) $CXCR4^{f/f}$ and CXCR4 WT genes. (E) Genotyping PCR results of Cre + $CXCR4^{f/f}$ and Cre-$CXCR4^{f/f}$ mice after tamoxifen injection demonstrating the recombined CXCR4 deleted gene construct in Cre + CXCR4f/f mouse but not in Cre-CXCR4f/f control. (F and G) Relative CXCR4 mRNA expression levels normalized to GAPDH in control mice and CXCR4KO mice in (F) peripheral blood and (G) bone marrow cells. $n = 8$ mice/group. (H) In vitro transwell migration assay of BM cells showing representative images of BM cells from control mice and CXCR4KO mice migrated towards CXCL12 ligand at various concentrations (0, 30, or 100 ng/mL). (I) Quantitative summary of transwell migration assay showing the chemotactic index of BM cells of control mice and CXCR4KO mice towards CXCL12 ligand at various concentrations. In vitro data in H-I are representative of three independent experiments. Data in bar graphs are shown as mean ± SEM. $^{*}P < 0.01$, $^{**}P < 0.001$.

Tamoxifen injection

Tamoxifen (Sigma-Aldrich) was dissolved in corn oil at a concentration of 20 mg/mL. Tamoxifen was administered to mice by intraperitoneal injection for five consecutive days (75 mg/kg). Retro-orbital blood was obtained two weeks after the last dose of tamoxifen to assay for Cxcr4 mRNA for determination of Cxcr4 downregulation in peripheral blood cells.

Processing of blood, BM, spleen, and uterus samples and flow cytometry analysis

Uterine implantation sites were extracted and fetal/placental parts were removed from the uterus as previously described [23]. In nonpregnant mice, one uterine horn was extracted for flow cytometry processing. Uterine tissues were finely minced and subsequently digested with a solution of Hanks balanced salt solution (Life Technologies, Inc) containing collagenase B (1 mg/mL; Roche Diagnostics), deoxyribonuclease I (0.1 mg/mL; Sigma-Aldrich), and 1% penicillin/streptomycin for 30–45 min at 37 °C. The cell suspension was filtered through a 70 μm filter and centrifuged at 2000 rpm for 8 min at 4 °C. The cell pellet was washed with PBS by centrifugation at 2000 rpm for 5 min at 4 °C and then resuspended in PBS with 2% fetal bovine serum (FBS) (FACS buffer). Bone marrow was flushed from tibias and femur bones with DMEM/F12 medium. The whole spleen was removed and crushed using mortar and pestle to extract splenic cells. Peripheral blood was obtained by retro-orbital venipuncture and collected into EDTA-coated tubes on ice. All samples were filtered using sterile 70 μm mesh and centrifuged at 2000 rpm at 4 °C for 5 min followed by red blood cell (RBC) lysis for 10 min at room temperature in RBC lysis buffer as per the manufacturer's protocol (Mltenyi Biotec). The cell suspensions were then washed two times by centrifugation and resuspended in FACS buffer. Total extracted cells per mouse were counted using a hemocytometer and 2×10^6 cells were resuspended in FACS buffer and incubated with mouse Trustain FcX PLUS anti CD16/32 blocking (Biolegend) for 10 min, followed by incubation with the appropriate antibodies at room temperature for 30 min. The cells were then washed three times with FACS buffer at 1500 rpm at 4 °C for 5 min and the pellet was resuspended in 500 μL ice-cold PBS for flow cytometry analysis. Flow cytometry was performed on LSRII Green (BD Biosciences). Gates were applied to forward-scatter/side-scatter dot plots to exclude nonviable cells and cell debris. Appropriate unstained and antibody IgG isotype controls were used for setting compensation and determining gates. Data were analyzed using the software FlowJo V10 (FlowJo). Antibodies used in flow cytometry analysis are listed in Supplementary Table S2.

Bone marrow MSC culture

BM cells were extracted from CXCR4iKO and control mice after BM was flushed from tibia and femur bones with DMEM/F12 medium and BM mesenchymal stem cells (MSC) cell culture was established as previously described [24]. Briefly, extracted BM cells were filtered through 70 um filter and centrifuged at 2000 rpm for 8 min at 4 °C, then resuspended in MSC expansion medium containing MesenCult Basal Medium, MesenCult 10X Supplement, MesenPure, L-Glutamine, 1% penicillin/streptomycin antibiotic (MesenCult Expansion Kit (Mouse), Stem Cell Technologies). Cells were counted and 5×10^7 cells were plated in T-75 flask in 15 ml MesenCult medium. They were cultured at 37 °C under 5% CO_2. After 1 week, cells were passaged and maintained until second passage (P2). P2 cells were used for subsequent flow cytometry characterization and RT-PCR.

Colony forming unit assay

BM cells were extracted from CXCR4iKO and control mice as described above. Freshly isolated BM cells were plated in 2 mL of complete MesenCult Expansion Medium (Stem Cell Technologies) per well of 6-well plate at a concentration of 5×10^5 cells/well. Cells were cultured at 37 °C, 5% CO_2 for a total of 14 days with half medium change performed after 7 days. After 14 days of culture, the medium was aspirated and the cells were washed with PBS, fixed in 4% PFA for 30 min, and washed with PBS two times. Cells were subsequently stained with 0.5% crystal violet in methanol for 15 min at room temperature followed by washing with distilled water three times prior to visualization. Colonies within each well were visualized and counted using Olympus BX-51 light microscope (Olympus). A colony forming unit (CFU) was defined as at least 40 cells. The assay was performed in triplicate with three independent experiments.

CXCL12 Transwell migration assay

BM cells were extracted from CXCR4iKO and control mice as described above. Migration assay to CXCL12 chemoattractant gradient was performed using 24-well transwell chemotaxis chamber inserts (pore size, 8 μm)(Corning Costar). DMEM/F12 medium (600 μL) containing recombinant mouse CXCL12 at different concentrations (0, 30, and 100 ng/mL) was placed in the lower chamber. A total of 1×10^4 BM cells in 200 μL DMEM/F12 medium were loaded into the upper chamber. They were then incubated for 4 h at 37 °C in 5% CO_2. Following incubation, the upper chambers were removed and the GFP + BM cells that had migrated to the lower chamber were visualized using GFP fluorescent camera and four high power field (HPF) random images were acquired. For quantification, the number of migrating cells in each HPF image was counted and averages of 4 HPFs were calculated per well. Each assay was performed in duplicate, and two independent experiments were carried out. Chemotactic index was calculated as a percentage (%) of the average number of migrated cells divided by the total number of cells plated.

RNA extraction and quantitative real-time polymerase chain reaction

Total RNA from peripheral blood, fresh BM cells or cultured BM cells was extracted by disrupting the cells with 300 μl RLT buffer containing β-mercaptoethanol followed by processing using the RNeasy Mini kit (Qiagen) according to the manufacturer's protocol. This was followed by treatment with DNase using the TURBO DNA-free kit (Life Technologies). For each sample, 500 ng of total RNA was reverse-transcribed with the iScript cDNA synthesis kit (Bio-Rad) according to the manufacturer's instructions. qPCR was performed using iQ SYBR Green Supermix (BioRad) on a Bio-Rad CFX96 thermocycler using the gene-specific primer pairs listed in Supplementary Table S1. Gene expression was analyzed on duplicate samples, and the Ct values were normalized to the internal control GAPDH housekeeping gene. The reaction

products were confirmed by 1.5% agarose gel electrophoresis and visualized by UV light after staining with ethidium bromide.

Immunohistochemistry and immunofluorescence

Uterine tissues were fixed in 4% paraformaldehyde and embedded in paraffin. Five-micrometer tissue sections were mounted on slides, followed by deparaffinization and rehydration. Slides were then boiled in sodium citrate (pH 6.0) for antigen retrieval. For immunohistochemistry, sections were blocked with 5% rabbit serum followed by incubating with primary goat anti-GFP antibody (1:1000, Abcam, CA) overnight at 4 °C. Sections were then incubated with biotinylated secondary antibody (1:200, Vector Laboratories) for 1 h. Detection was performed using ABC Vectastain Elite reagents with DAB plus H_2O_2 (Vector Laboratories). Tissue sections were counterstained with hematoxylin (Sigma-Aldrich). Images of stained sections were obtained using an Olympus BX-51 microscope (Olympus).

For immunofluorescence, blocking was done in 10% donkey serum for 1 h at room temperature. The slides were then incubated in the appropriate concentration of primary antibody overnight at 4 °C. The next morning the slides were washed and incubated with fluoroscein 488-conjugated DBA lectin, Alexa Fluor 568-conjugated donkey anti-goat and Alexa Fluor 647 donkey anti-rat (Life Technologies, San Francisco, CA) at room temperature for 1 h. Afterwards, Vectashield fluorescent mounting media with 4′,6-diamidino-2-phenylindole (DAPI) (Vector Laboratories) was applied for mounting and visualization of nuclear staining. Immunoreaction with amplification but without primary and/or secondary antibodies served as negative controls. Images were then taken using laser scanning confocal microscope (LSM 880 with Airyscan, Carl Zeiss) and analyzed using ZEN software. Primary and secondary antibodies and their respective concentrations used are listed in Supplementary Table S1.

Statistical analysis

All WT and CXCR4 KO mice were age matched. GraphPad Prism 8 software (GraphPad Software, La Jolla, CA) was used for statistical analysis. Data were assessed for normal distribution with a Shapiro–Wilk normality test. Normally distributed data were analyzed using the Student unpaired two-tailed *t* test for the comparison of two groups, and one-way ANOVA with Tukey multiple comparison test for multiple group comparison. If data were not normally distributed, or if distribution could not be determined due to small sample size, data were analyzed using a Mann–Whitney U test. $P < 0.05$ was considered statistically significant. All data are reported as mean ± SEM.

Results

Establishment and validation of BM-specific CXCR4 knockout model

To study the role of CXCR4 in BM cells in the recruitment of BM-derived nonhematopoietic progenitor cells to the uterus both during pregnancy and in the nonpregnant state, we generated mice that have inducible CXCR4 knockout using the Cre-LoxP system. We used tamoxifen-inducible knockout system to induce the knockout (CXCR4KO) in adulthood since CXCR4 knockout results in embryonic lethality [29, 30]. The CXCR4KO mice also harbor the *GFP* transgene allowing us to track the transplanted BM cells. Genotyping of the *Cre/ESR1* transgene and $CXCR4^{flox/flox}$ gene are shown in Figure 1C and D. All experiments were initiated following 14-day washout period from the last dose of tamoxifen administration. Successful ablation of *CXCR4* gene following tamoxifen administration in $Cre^{+}CXCR4^{flox/flox}/GFP^{+}$ mice (generating CXCR4KO mice) was confirmed by the presence of the deleted CXCR4 KO-only product (Figure 1E). We validated the tamoxifen-inducible CXCR4 deletion in CXCR4KO mice in peripheral blood cells and BM cells by quantitative RT-PCR showing >90% reduction in *Cxcr4* mRNA expression in CXCR4KO mice compared to the control group (Figure 1F and G). Body weight was not affected by CXCR4 ablation (data not shown). As further functional validation of CXCR4 KO, we examined the chemotactic behavior of BM cells in response to CXCL12. Freshly isolated BM cells from CXCR4KO and WT control mice (both expressing GFP) were cultured in transwell plates and treated with varying concentrations of CXCL12 to induce migration, and GFP-labeled cells on the underneath surface of the membrane were quantified (Figure 1H and I). CXCL12 resulted in 1.4-fold ($P < 0.05$) and 1.9-fold ($P < 0.01$) increase in chemotactic index of BM cells at concentrations of 30 ng/ml and 100 ng/mL CXCL12, respectively, in the control BM cells. In contrast, no increase in chemotaxis was observed in BM cells from CXCR4KO mice at 30 and 100 ng/mL concentrations of CXCL12, indicating that the ability of BM cells to migrate in response to CXCL12 stimulus is abolished in CXCR4 knockout compared to control WT mice (Figure 1H and I). Collectively, these data confirmed a successful construction of a CXCR4 knockout mouse , which can be utilized for further analyses.

CXCR4 ablation affects recruitment of bone marrow-derived cells to the pregnant uterus

After validating the efficiency of the CXCR4 knockout in our mouse model, we wished to investigate the effects of CXCR4 knockout in BM cells on recruitment of BMDCs to the pregnant uterus. First, we characterized the numbers and properties of BM MSCs in CXCR4KO mice. Freshly isolated BM from CXCR4KO and WT control mice was extracted and cultured adherently in MSC media. Multicolor flow cytometry of cultured BM cells revealed no difference in the percentage of cells expressing established MSC markers ($Sca\text{-}1^{+}CD29^{+}CD44^{+}$) but negative for the hematopoietic marker CD45 ($CD45^{-}$) between CXCR4KO and control mice (Figure 2A), suggesting that there is no numerical difference in BM MSCs following CXCR4 KO. Moreover, CFU assay showed that BM MSCs from CXCR4KO mice have significantly higher clonogenic capacity compared with control mice, as demonstrated by their greater ability to form colonies (Figure 2C and D). In addition, gene expression of stem cell markers *Oct4, Nanog* and *Sox2* as well as *Cxcl12*, and BM MSC-specific marker *Hoxa11* [31] were not different in cultured MSCs after CXCR4 knockout (Figure 2E).

To investigate the potential role of CXCR4 in recruitment of BMDCs to the pregnant decidua, we established chimeric mice with BM-specific CXCR4 KO by nongonadotoxic submyeloablation followed by transplantation of BM cells from $Cre^{+}CXCR4^{fl/fl}$ mice into WT recipients, with subsequent tamoxifen administration (Figure 1B). The CXCR4KO mice also harbor the GFP transgene allowing to track the

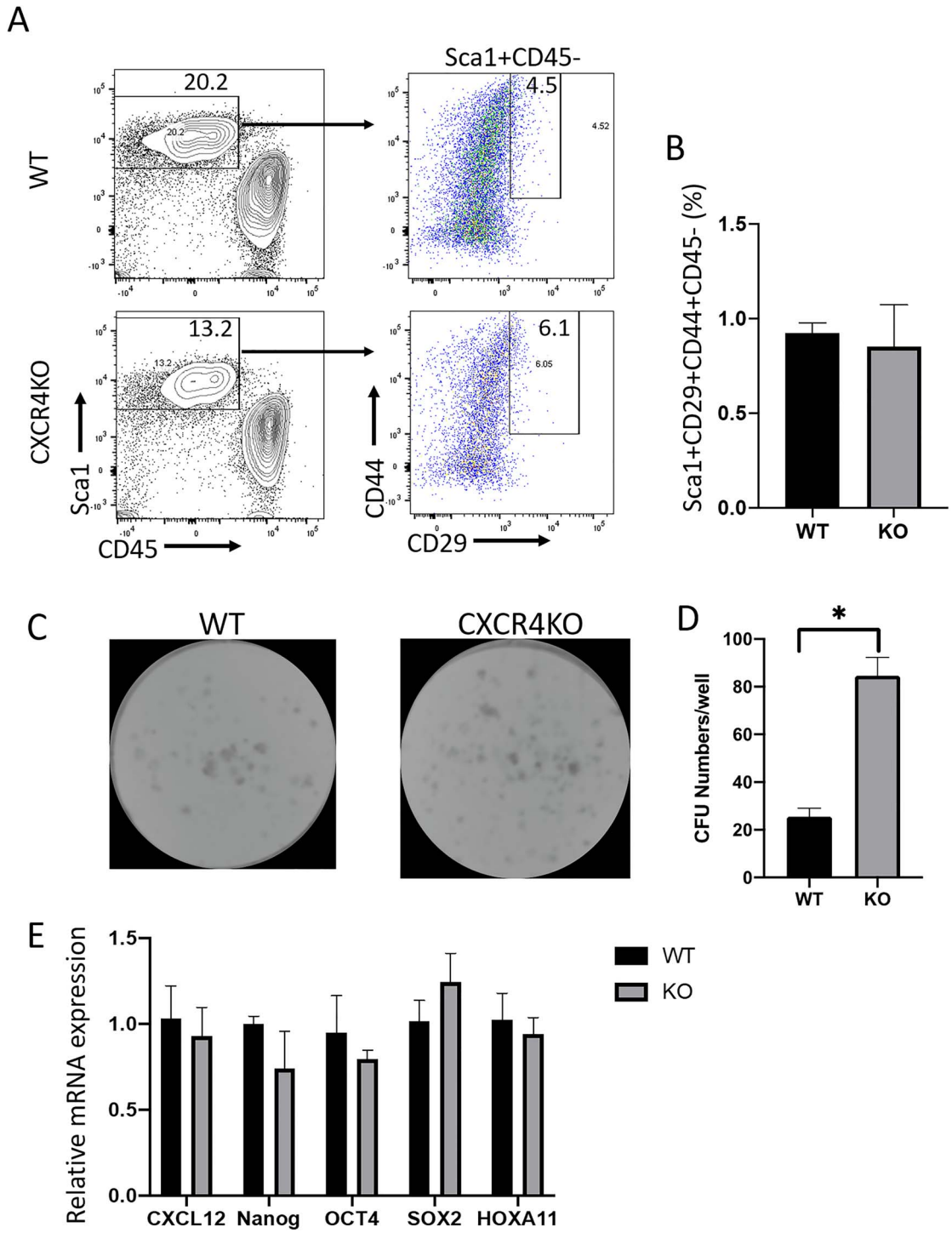

Figure 2. (A) Multicolor flow cytometry analysis of cultured BM cells from CXCR4KO and control mice. Live cells were gated on Sca-1+ and CD45– to exclude hematopoietic cells, and were further gated on CD29+ and CD44+ to identify BM MSCs. Representative flow cytometry plots of cultured BM cells are shown. (B) Quantitative summary of percentage of CD29+/CD44+/Sca1+/CD45– BM MSCs in CXCR4KO and control mice. Data shown in (A) and (B) are the mean of $n = 4$ mice/group. (C) CFU assay showing representative images of colony development in cultured BM cells of CXCR4KO and control mice. (D) Quantitative summary of CFU numbers per well in CXCR4KO and control mice. $^*P < 0.01$, $n = 4$ mice/group. (E) Quantitative summary of mRNA expression of Cxcl12, Nanog, Oct4, Sox2, and Hoxa11 in cultured MSCs of CXCR4KO and control mice. CFU assays and quantitative real-time polymerase chain reaction assays were performed in duplicate and data are the averages of two independent experiments. Data in bar graphs are shown as mean ± SEM.

transplanted BM cells. For BMT, we utilized our previously described 5-FU-based nongonadotoxic submyeloablation BMT regimen which maintains fertility in the mice [22–24]. Since CXCR4 is essential for engraftment and retention of BM cells in the BM [4], tamoxifen administration to induce CXCR4 KO was designed to be after and not prior to BM transplantation to facilitate normal engraftment of donor BM. Successful donor BM engraftment was confirmed

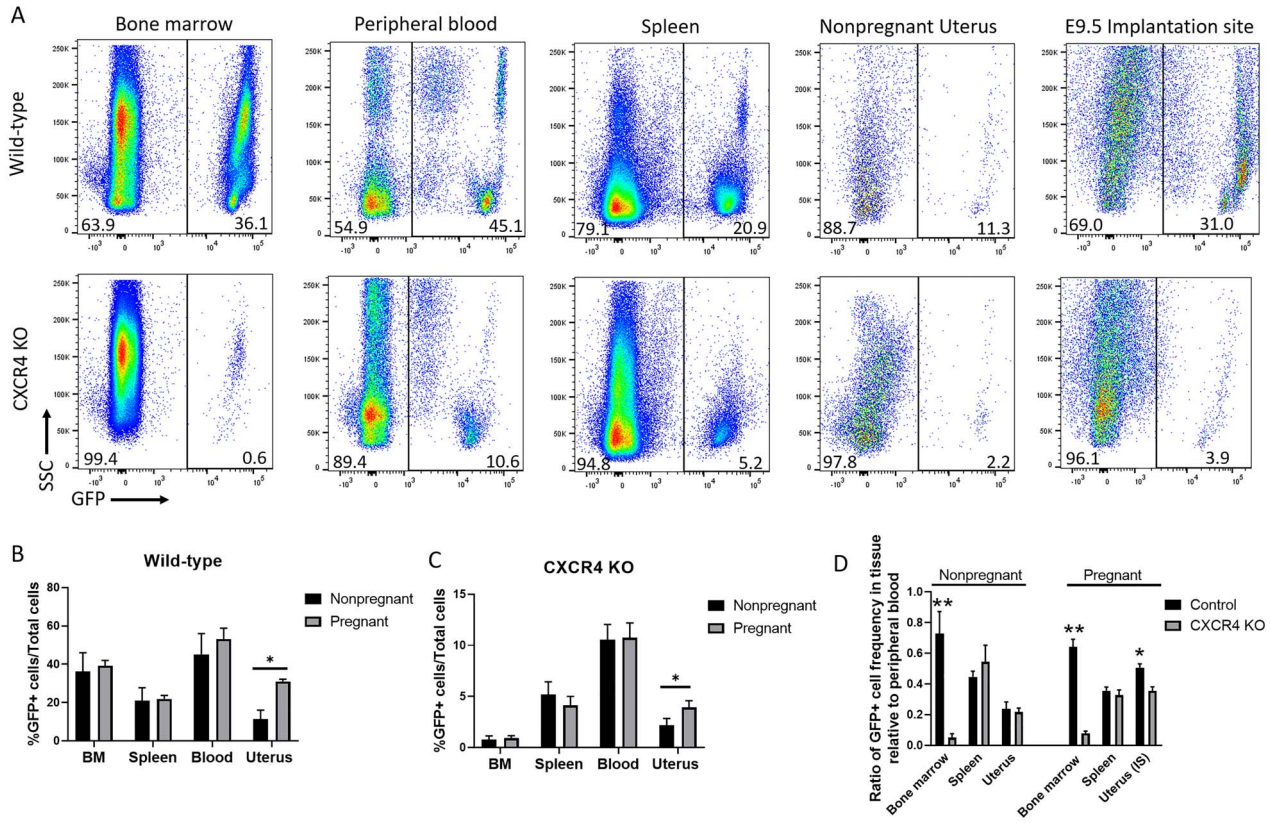

Figure 3. (A) Flow cytometry analysis showing GFP+ cells in bone marrow, peripheral blood, spleen, nonpregnant uterus, and decidua (E9.5) of CXCR4KO and WT control mice. Live cells were gated on GFP to calculate the percentage of BMDCs (GFP+). Representative flow cytometry plots are shown. (B and C) Quantitative summaries of percentage of GFP+ cells present in bone marrow, spleen, blood, and uterus in (B) WT control and (C) CXCR4KO mice in both pregnant (E9.5) and nonpregnant samples. (D) Quantitative summary of the ratio of GFP+ cell frequency in bone marrow, spleen, and uterus relative to peripheral blood in control and CXCR4KO mice in both pregnant (E9.5) and nonpregnant samples. $n = 6$ mice/group, $^{*}P < 0.05$, $^{**}P < 0.01$. Data in bar graphs are shown as mean ± SEM.

by flow cytometry analysis of peripheral blood on day 21 post-BMT (Supplementary Figure S1), consistent with our previous experience using this model [24]. WT recipients of BM from $Cre^{-}CXCR4^{fl/fl}$ donor mice followed by tamoxifen administration served as controls and are hereby referred to as WT. Two weeks following tamoxifen administration, peripheral blood from the mice was assayed for *Cxcr4* mRNA expression and confirmed partial downregulation (~44%) of *Cxcr4* in CXCR4KO mice as compared to WT (Supplementary Figure S1). After mating and establishing timed pregnancies, we analyzed the pregnant decidua or nonpregnant uterus, BM, peripheral blood, and spleen either on E9.5 or on nonpregnant (estrus) timepoints by flow cytometry for quantitating GFP+ BMDCs in the tissues. The percentage of GFP+ cells was strikingly lower in BM of CXCR4KO mice as compared to other organs examined as well as compared to control mice (Figure 3A–C), consistent with the known role of CXCR4 expression on BM cells in their retention within the BM niche. A significant increase in the percentage of GFP+ cells was noted in the uterine implantation site as compared to the nonpregnant uterus in WT (2.7-fold) and to a lesser extent in CXCR4KO (1.8-fold) mice (Figure 3A–C). This pregnancy-induced increase was specific to the uterus tissue and was not observed in BM, peripheral blood and spleen tissues of either experimental groups (Figure 3A–C). Notably, the ratio of GFP+ cell frequency in BM relative to peripheral blood was lower in CXCR4KO compared to controls in both pregnant and nonpregnant mice (Figure 3D). The ratio of GFP+ cell frequency in uterine tissue relative to peripheral blood was also lower in CXCR4KO compared to controls specifically in pregnant mice but not in nonpregnant mice (Figure 3D), indicating decreased recruitment of BMDCs to the uterus in pregnancy in CXCR4KO mice. In contrast, the ratio of GFP+ cell frequency in spleen and nonpregnant uterus relative to peripheral blood was not different in CXCR4KO compared to controls in either pregnant and nonpregnant mice (Figure 3D). Immunostaining of histological uterine sections with GFP antibody were consistent with our flow cytometry data, demonstrating overall decreased numbers of GFP+ BMDCs in CXCR4KO uteri in both pregnant (E8.5) and nonpregnant states (Figure 4A and B). In the nonpregnant uterus, GFP+ BMDCs were primarily localized in the endometrial stroma and to a lesser extent in the myometrium. No GFP+ cells were found in endometrial luminal or glandular epithelium. In pregnancy, GFP+ BMDCs were specifically concentrated in the maternal decidua on the mesometrial side and absent from the embryonic tissues (embryo, trophoblast) (Figure 4B). GFP+ BMDCs were mostly localized in the stroma within the mesometrial area of the implantation site (Figure 4B). We did not observe any differences in the number of implantations and resorptions in the

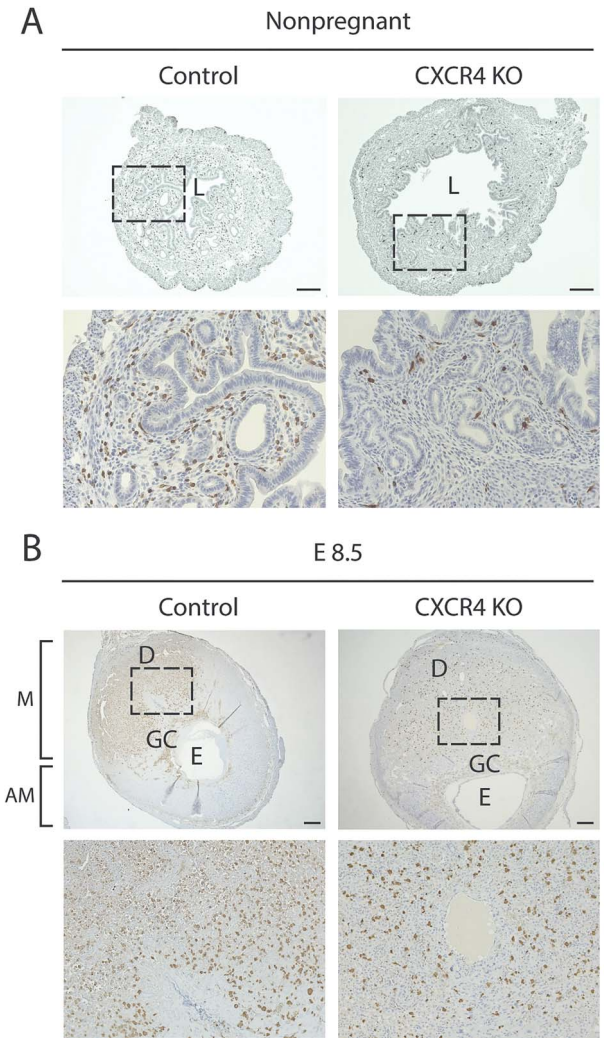

Figure 4. Immunohistochemistry images of uterine tissue sections from CXCR4KO and control mice. (A) Immunostaining images of nonpregnant uterine tissue sections of control and CXCR4KO stained with GFP antibody (brown). The bottom panel (20×) is a magnification of the dashed area in the upper panel (4×). Scale bar, 200 μm. (B) Immunostaining images of implantation site (E8.5) sections of control and CXCR4KO stained with GFP antibody (brown). The bottom panel (10x) is a magnification of the dashed area in the upper panel (2.5×). Note the concentration of GFP+ BMDCs in the mesometrial (M) area compared to the scant presence in the antimesometrial (AM) area. L, lumen; GC, giant cell layer; E, embryo. Scale bar, 400 μm.

CXCR4KO mice as compared to WT control mice (data not shown).

CXCR4 mediates recruitment of bone marrow-derived nonhematopoietic cells to the pregnant uterus

To investigate whether recruitment of nonhematopoietic and hematopoietic cells to the pregnant uterus is similarly affected by knockout of CXCR4 in BM, we analyzed single uterine cells by flow cytometry using antibody to CD45 (panleukocyte marker). Flow cytometry analysis demonstrated an increase in both hematopoietic (CD45+) and nonhematopoietic (CD45–) GFP+ BMDCs in control mice comparing nonpregnant uterus to pregnancy implantation site (Figure 5A and B). In contrast, in CXCR4KO mice there was an increase in hematopoietic BMDCs in the uterus in pregnancy compared to the nonpregnant uterus, while there was no increase in nonhematopoietic BMDCs in the pregnant uterus compared to nonpregnant (Figure 5A and C). We confirmed this finding using immunofluorescence colocalization analysis. Since NK cells are the most abundant hematopoietic population in the implantation site, peaking on E8.5–E9.5 [32], we performed co-staining of GFP together with CD45 (panleukocyte) and DBA (*Dolichos biflorus* lectin) lectin, a specific marker of NK cells. DBA lectin is the commonly used marker for mouse uterine NK cells as it stains both cytoplasmic granules as well as the cell membrane, thus identifying also immature, agranular NK cells [33]. Moreover, DBA lectin is consistently found on BM-derived NK cells that have homed to the uterus [33]. Immunostaining demonstrated that in both control mice and CXCR4KO mice, most GFP+ BMDCs were CD45+ and DBA+, indicating that they were BM-derived NK cells (Figure 6A and B). A minority of GFP+ cells were positive for the CD45+ hematopoietic marker but negative for DBA, indicative of non-NK immune cells. In control mice, immunofluorescence colocalization also showed the presence of GFP+/CD45–/DBA– cells, indicative of BM-derived nonhematopoietic cells. Notably, these nonhematopoietic GFP+ cells were not found in implantation sites of CXCR4KO mice (Figure 6A and B).

CXCR4 ablation differentially affects recruitment of immune cell population subsets to the pregnant uterus

To determine the effects of CXCR4 knockout on the dynamics of various BM-derived hematopoietic immune cell subsets, we performed multicolor flow cytometry analysis of bone marrow, spleen, peripheral blood and implantation site (E9.5) tissues. Single live cells were gated on GFP+ and CD45+ hematopoietic cells (Figure 7A). Among hematopoietic BMDCs, there was a decrease in the proportion of myeloid cell populations in the spleen, peripheral blood and implantation site of CXCR4KO as compared to controls animals (Figure 7B–E). The percentages of neutrophil and monocyte subsets out of total hematopoietic BMDCs were decreased in implantation site, spleen and peripheral blood but were unaffected in BM of CXCR4KO mice versus WT controls. The percentage of macrophages out of total hematopoietic BMDCs were also decreased in the implantation site of CXCR4KO mice compared to controls (Figure 7D). Moreover, significant alterations were observed in proportions of lymphoid cell populations in CXCR4KO animals. The proportion of T cells out of total hematopoietic cells were increased in spleen and peripheral blood but unchanged in BM and implantation site of CXCR4KO mice vs. controls (Figure 7B–E). The percentage of NK cell subset out of total hematopoietic cells was increased in the implantation site and BM but decreased in spleen and peripheral blood in CXCR4KO vs. control mice (Figure 7B–E). When immune cell frequencies at the implantation site, spleen, and bone marrow were assessed as a ratio relative to their frequency in the peripheral blood, it revealed a striking increase in the ratio of NK cells at the implantation site relative to blood (24-fold) in CXCR4KO mice as compared to control mice (1-fold) and to all other tissues (Figure 7F), suggesting that CXCR4 is not required for recruitment and accumulation of BM-derived NK cells in the implantation site. In addition, there was a higher

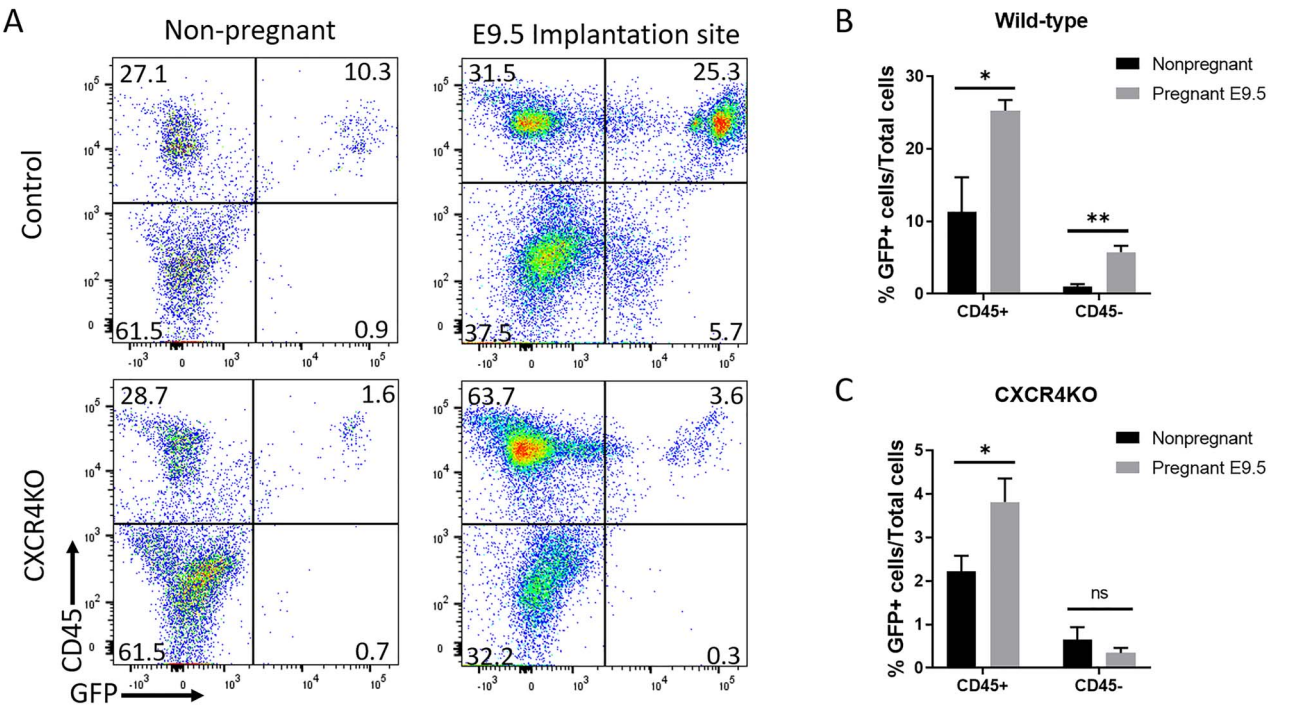

Figure 5. (A) Flow cytometry analysis of nonpregnant uterus and decidua (E9.5) from control and CXCR4KO mice. Live cells were gated on GFP and CD45 to identify GFP$^+$CD45$^+$ hematopoietic BMDCs and GFP$^+$CD45$^-$ nonhematopoietic BMDCs. Representative flow cytometry plots are shown. (B and C) Quantitative summary of percentage of GFP$^+$CD45$^+$ hematopoietic BMDCs and (C) GFP$^+$ CD45$^-$ nonhematopoietic BMDCs in nonpregnant uterus and implantation site (E9.5) of (B) control and (C) CXCR4KO mice. $n = 6$ mice/group, $^*P < 0.05$, $^{**}P < 0.01$. Data in bar graphs are shown as mean ± SEM.

ratio of neutrophils relative to blood in the BM (10-fold) of CXCR4KO mice vs. controls (Figure 7F).

Discussion

Adult BMDPCs have been shown to migrate to the uterus in both human [34–36] and mouse [22–24, 35, 37–40] and contribute to various nonhematopoietic cells of the endometrium including stromal, endothelial and epithelial compartments. Despite their identification in endometrial homeostasis, the role of these cells in highly dynamic physiological reproductive processes such as pregnancy and postpartum has remained unknown until recently [23–25]. Nonhematopoietic BM progenitors are mobilized to the circulation in pregnancy and recruited to the pregnant uterus where they give rise to decidual stromal cells, playing an important functional role in decidualization and pregnancy maintenance [23, 41]. Our study demonstrates an essential role for CXCR4 signaling in pregnancy-induced recruitment of nonhematopoietic BMDPCs to the decidua.

In the present study, we observed that the migration of BM-derived hematopoietic cells and nonhematopoietic cells to the uterus was significantly increased upon pregnancy in WT mice, consistent with our prior observations [23–25]. In contrast, the pregnancy-induced recruitment of BM-derived nonhematopoietic cells to the uterus was abolished while the recruitment of hematopoietic cells was also decreased when CXCR4 receptor was genetically ablated in BM cells. The CXCL12–CXCR4 axis is well established as playing a key role in recruitment of BM-derived stem cells [7, 42]. The expression of CXCL12 increases in response to tissue injury in various organs where it recruits MSCs to the damaged areas facilitating tissue repair [43–45]. Expression of CXCR4 receptor on the surface of BM MSCs has been shown to mediate their recruitment into areas of tissue injury in the setting of ischemic myocardial and brain injury and acute kidney injury [46–48]. Previously, CXCL12 ligand and its CXCR4 receptor have been shown to be important in mediating migration of BMDPCs towards endometrial stromal cells and myometrial stromal cells in vitro [15, 21, 49]. In addition, the CXCL12 ligand can increase while the CXCR4 antagonist AMD3100 can decrease the recruitment of BMDPCs to the uterus in vivo in a mouse uterine injury (Asherman's) model, with an increase in BMDPCs recruitment correlated to improved pregnancy outcome [50]. The results of the current study are consistent with these studies, pointing to an essential role of CXCR4 in mediating recruitment of nonhematopoietic BMDPCs to the decidua during pregnancy.

Loss of CXCR4 signaling in BM MSCs by genetic ablation in our study resulted in increased CFU ability but had no appreciable effects on the absolute number of BM-MSCs propagated in adherent culture. This is consistent with a prior mouse study showing that CXCR4 gene ablation in mature osteoblasts similarly led to increased number of colony-forming units in BM stromal cell cultures, that was associated with decreased bone mass and alterations in bone structure [51].

In this study, the number of transplanted donor-derived BM cells (GFP+) was profoundly lower in the BM niche of mice with CXCR4KO BMT as compared to WT. Although a decrease in donor-derived BM cells was observed in other organs (spleen, blood, implantation site) in CXCR4KO mice, donor-derived BM cells were most severely reduced

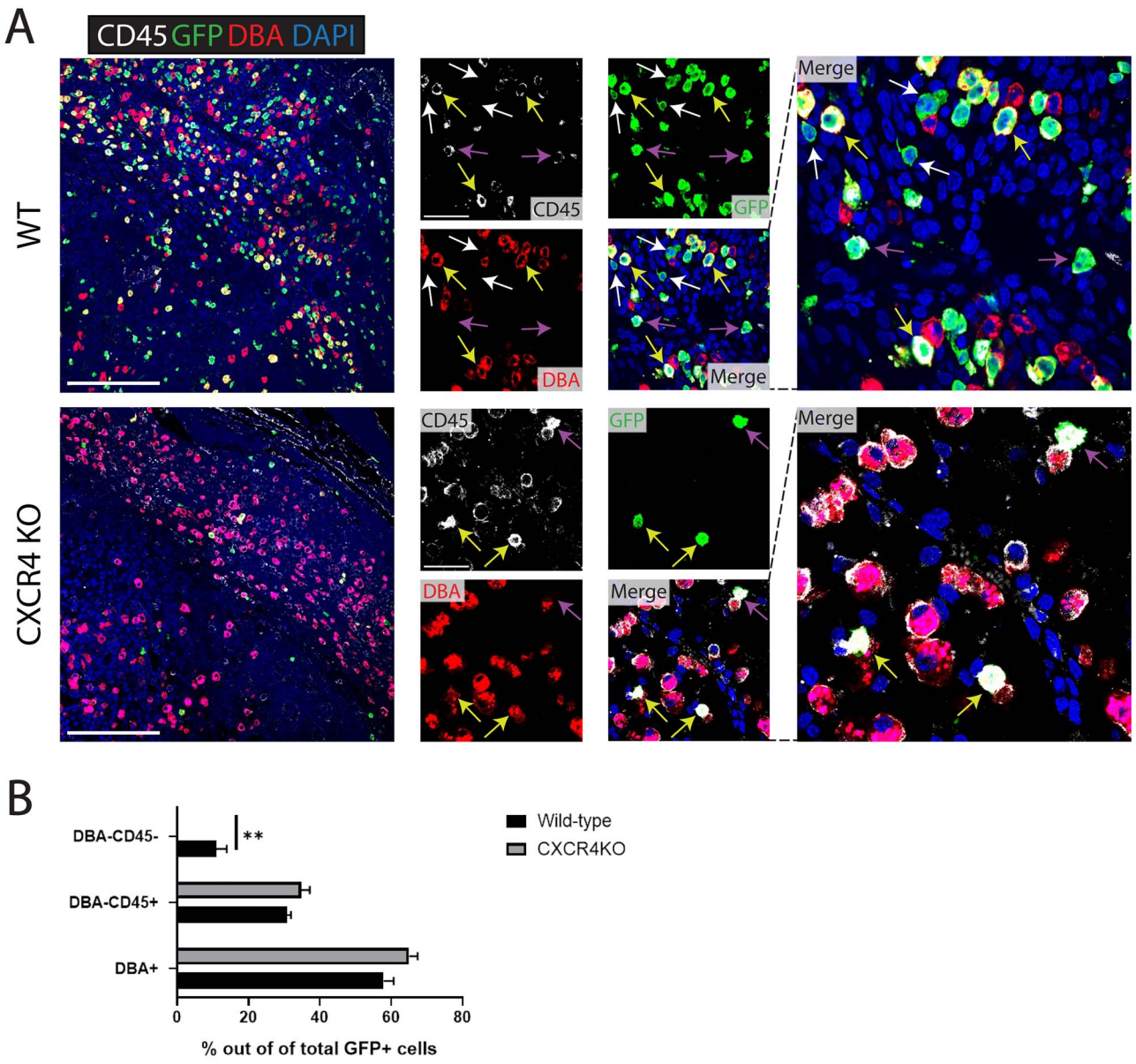

Figure 6. (A) Immunofluorescence of E9.5 decidua tissue sections (mesometrial) showing colocalization of CD45 pan-leukocyte marker (white), GFP marker of transplanted BMDCs (green), and DBA marker of NK cells (red) in control and CXCR4KO mice. Sections were counterstained with DAPI for nuclear staining (blue). White arrows point to nonhematopoietic GFP+ BMDCs that are negative for either CD45 or DBA markers. Yellow arrows point to GFP + CD45 + DBA+ BM-derived NK cells. Purple arrows point to GFP + CD45 + DBA– BM-derived non-NK immune cells. Note that nonhematopoietic GFP+ BMDCs (GFP + CD4 – DBA–) are found in control mice (white arrows) but not in CXCR4KO mice, where all GFP+ BMDCs are hematopoietic (CD45+ and/or DBA+). Low magnification picture scale bar, 200 μm. High magnification picture scale bar, 50 μm. (B) Quantitative summary of percentage of DBA+ (NK), DBA– CD45+ (immune non-NK) and DBA-CD45- (nonhematopoietic) BMDCs out of total GFP+ cells in the implantation site (E9.5) of control and CXCR4KO mice. $n = 4$ mice/group, $^{**}P < 0.01$. Data in bar graphs are shown as mean ± SEM.

in the BM. Since BM cell transplantation occurred prior to tamoxifen induction of genetic CXCR4 ablation, and initial donor BM cell engraftment was the same in both groups, the rapid decrease in donor-derived cells in the BM following CXCR4 ablation likely reflects rapid egress from the BM, consistent with the role of CXCR4 in retention of BM hematopoietic stem/progenitor cell within the BM niche [4]. Indeed, prolonged (>2 weeks) pharmacologic blockade of CXCR4 signaling leads to increased mobilization of stem cells from the BM [52]. Moreover, the mice with CXCR4KO BMT exhibited abnormally reduced proportions of certain donor-derived hematopoietic cells in hematopoietic organs including the spleen and peripheral blood with a decrease in myeloid (granulocyte, monocyte) and NK cell subpopulations. This is consistent with prior studies showing that CXCR4 in hematopoietic cells is essential for long-term lymphoid and myeloid reconstitution. Irradiated mice reconstituted with CXCR4-null fetal liver have reduced numbers of monocytic cells and granulocytic cells in hematopoietic organs [53, 54]. In addition, mice with conditional deletion of CXCR4 in adulthood have been shown to have decreased numbers of NK progenitor cells and mature NK cells in bone marrow, spleen and peripheral blood [55]. In contrast to myeloid and NK cell subpopulations that were decreased in hematopoietic organs

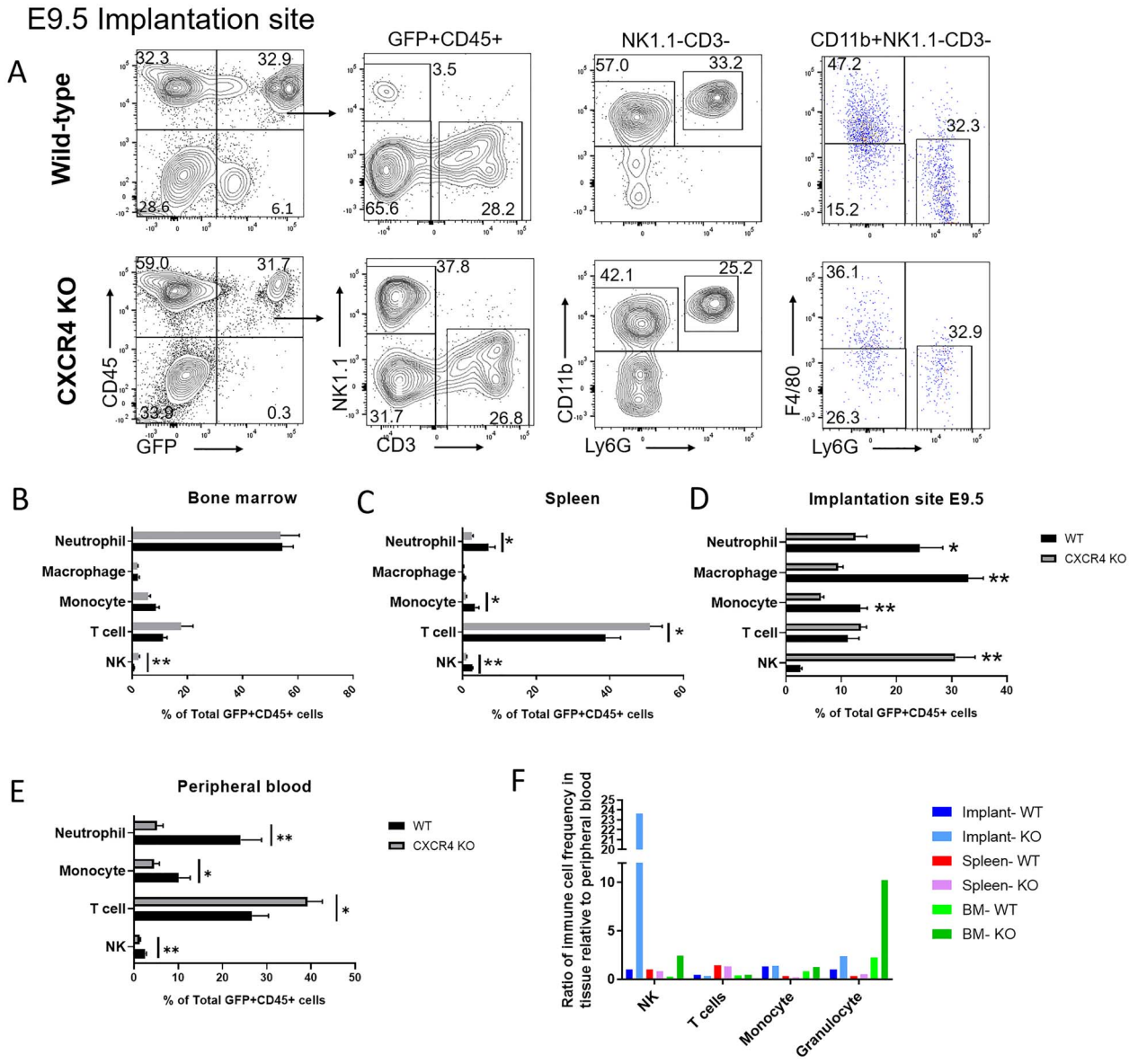

Figure 7. Multicolor flow cytometry analysis of GFP+ BM-derived hematopoietic cells in nonpregnant and pregnant (E9.5) mice tissues. (A) Gating strategy for flow cytometry analysis of GFP+ cells in implantation site (E9.5) of control and CXCR4KO mice. Live cells were gated on CD45+ and GFP+ to analyze the hematopoietic BMDC population. NK cells were positive for Nk1.1 (NK) but negative for CD3 (T cell) markers, while T cells were CD3+ NK1.1–. Cells were further gated as NK1.1–CD3– to analyze myeloid cells. The markers CD11b, Ly6G, and F4/80 were used to identify granulocytes (Ly6G+ CD11b+ F4/80–), macrophages (F4/80+ CD11b+ Ly6G–), and monocytes (CD11b+ F4/80– Ly6G–). Representative flow cytometry plots of single cells from E9.5 decidual tissue are shown. (B–E) Quantitative summary of the distribution of various immune cell subsets (neutrophils, macrophages, monocytes, T cells, and NK cells) in GFP$^+$ CD45$^+$ hematopoietic BMDCs of control and CXCR4KO mice in (B) bone marrow, (C) spleen, (D) implantation site, and (E) peripheral blood. (F) Quantitative summary of ratio of immune cell frequency (NK cells, T cells, monocytes, and granulocytes) in tissue (decidua, BM, or spleen) relative to peripheral blood in control and CXCR4KO mice. Data shown are the mean of $n = 6$ mice/group; $^*P < 0.05$, $^{**}P < 0.01$. Data in bar graphs are shown as mean ± SEM.

in our study, T cells were conserved and were proportionately increased. This is also consistent with prior studies showing that CXCR4 deletion does not impair T-cell precursors and does not influence localization of T lymphocytes in secondary lymphoid organs [54, 55].

We observed a striking increase in the ratio of NK cells at the implantation site relative to peripheral blood (24-fold) in CXCR4KO mice as compared to control mice (1-fold) and to all other tissues examined. Previous studies have shown that successful transition of the cycling endometrium to a pregnancy state requires selective elimination of proinflammatory senescent decidual cells by activated uterine NK cells [56]. Recurrent pregnancy loss, however, is characterized by a deficiency in endometrial MSCs and increased decidual cell senescence [57–59]. Therefore, it is very plausible that the vast relative increase in decidual NK cells in CXCR4KO mice represents a compensatory response to the BMDPC deficiency.

The role of CXCL12/CXCR4 pathway in embryo implantation and placentation is implicated by several lines of evidence. The CXCR4 receptor and its CXCL12 ligand have been shown to be upregulated in the endometrium of humans,

sheep and pigs during early pregnancy [13, 14, 60]. The CXCL12 ligand is highly expressed in endometrial epithelial and stromal cells [14–16], while its CXCR4 receptor is localized in stromal cells, vascular endothelial cells, and immune cells in the endometrium [14], as also revealed by recent single-cell transcriptomic data of human endometrium and maternal-fetal interface [61, 62]. Moreover, single-cell RNA-seq data showed that CXCL14 is the most abundant chemokine expressed in the human endometrium. Interestingly, CXCL14 is a positive allosteric modulator of CXCR4 that synergizes with CXCL12 [63, 64], and thus may play an important role in local amplification of CXCL12-CXCR4 pathway-mediated effects. CXCR4 also has essential roles in the cross-talk between trophoblast cells, maternal decidual cells and maternal immune cells by recruiting immune cells into the decidua and stimulating trophoblast proliferation and invasion [18, 19, 65]. CXCL12 can bind CXCR4 on decidual cells leading to increased activity of matrix metalloproteases (MMP) 2 and 9 [66], both of which are critical determinants for trophoblast migration and invasion [67]. Moreover, CXCL12 derived from embryonic tissue has been recently shown by Koo et al. to have beneficial effects on endometrial receptivity and embryo implantation [68]. Embryonic-derived CXCL12 led to increased embryo attachment and angiogenesis in-vitro, and intrauterine administration of CXCL12 resulted in increased expression of endometrial receptivity markers (integrin $\beta 3$, Osteopontin) and embryo implantation in vivo [68]. In addition, a recent randomized, placebo-controlled pilot trial demonstrated that sitagliptin, an oral antidiabetic drug and DPP4 inhibitor that increases CXCL12 bioavailability, is effective in increasing the number of clonogenic MSCs in the endometrium and attenuating the prosenescent decidual response in patients with recurrent pregnancy loss [69].Activation of CXCR4 by CXCL12 promotes CD4+ T cell survival [70], and also induces the recruitment of CXCR4+ T regulatory cells (CD4 + CD25+) to the pregnant uterus and prevents embryo loss in mice [20], suggesting that the CXCL12-CXCR4 system is involved in immune cell trafficking into the uterus to aid in establishment and maintenance of maternal tolerance to the semiallogenic fetus. Our study extends the role of CXCR4 to trafficking of nonhematopoietic BMDPCs into the uterus in pregnancy. Ultimately, the secretion of CXCL12 by decidual cells may serve as a mechanism to regulate proper trafficking of exogenous BM-derived immune and nonimmune cell populations to the decidua which, in turn, support implantation and pregnancy maintenance. Since our mouse model was a chimeric, we could not comment on the functional effects of inhibiting CXCR4 expression on BMDPCs in terms of implantation and pregnancy. However, BMDPC have been shown to have a functional role in supporting implantation and pregnancy maintenance [23], and it would be interesting to further explore the specific role of CXCR4 inhibition in BMDPCs on pregnancy outcome.

In conclusion, our results indicate that CXCR4 is essential for recruitment of BM-derived nonhematopoietic progenitor cells to the pregnant uterus. Genetic ablation of CXCR4 signaling in BM cells affects accumulation of myeloid cell populations but not NK cells in the pregnant uterus. These findings provide important insights into the regulation of BMDPCs trafficking into the uterus during pregnancy, that may have an important role in implantation and pregnancy maintenance.

Supplementary material

Supplementary material is available at *BIOLRE* online.

Data availability

The data underlying this article are available in the article and in its online supplementary material.

Authors' contribution

The authors have made the following declarations about their contributions: R.T. and H.S.T conceived the study and designed the research. Y-Y.F., F.L., N.A., A.T., and A.Y.C. performed the experiments. Y-Y.F. and F.L. analyzed the data. Y-Y.F. wrote the manuscript draft. R.T. revised the manuscript.

Conflict of interest

All of the authors declare no potential conflict of interest.

References

1. Fievez V, Szpakowska M, Mosbah A, Arumugam K, Mathu J, Counson M, Beaupain N, Seguin-Devaux C, Deroo S, Baudy-Floc'h M, Chevigné A. Development of mimokines, chemokine N terminus-based CXCR4 inhibitors optimized by phage display and rational design. *J Leukoc Biol* 2018; **104**:343–357.
2. Hersh TA, Dimond AL, Ruth BA, Lupica NV, Bruce JC, Kelley JM, King BL, Lutton BV. A role for the CXCR4-CXCL12 axis in the little skate, *Leucoraja erinacea*. *Am J Physiol Regul Integr Comp Physiol* 2018; **315**:R218–r229.
3. Karpova D, Bonig H. Concise review: CXCR4/CXCL12 signaling in immature hematopoiesis–lessons from pharmacological and genetic models. *Stem Cells* 2015; **33**:2391–2399.
4. Broxmeyer HE, Orschell CM, Clapp DW, Hangoc G, Cooper S, Plett PA, Liles WC, Li X, Graham-Evans B, Campbell TB *et al.* Rapid mobilization of murine and human hematopoietic stem and progenitor cells with AMD3100, a CXCR4 antagonist. *J Exp Med* 2005; **201**:1307–1318.
5. Sugiyama T, Kohara H, Noda M, Nagasawa T. Maintenance of the hematopoietic stem cell pool by CXCL12-CXCR4 chemokine signaling in bone marrow stromal cell niches. *Immunity* 2006; **25**: 977–988.
6. Murdoch C. CXCR4: chemokine receptor extraordinaire. *Immunol Rev* 2000; **177**:175–184.
7. Nagasawa T, Hirota S, Tachibana K, Takakura N, Nishikawa S, Kitamura Y, Yoshida N, Kikutani H, Kishimoto T. Defects of B-cell lymphopoiesis and bone-marrow myelopoiesis in mice lacking the CXC chemokine PBSF/SDF-1. *Nature* 1996; **382**:635–638.
8. Nie Y, Waite J, Brewer F, Sunshine MJ, Littman DR, Zou YR. The role of CXCR4 in maintaining peripheral B cell compartments and humoral immunity. *J Exp Med* 2004; **200**:1145–1156.
9. Lai CY, Yamazaki S, Okabe M, Suzuki S, Maeyama Y, Iimura Y, Onodera M, Kakuta S, Iwakura Y, Nojima M *et al.* Stage-specific roles for CXCR4 signaling in murine hematopoietic stem/progenitor cells in the process of bone marrow repopulation. *Stem Cells* 2014; **32**:1929–1942.
10. Page M, Ridge L, Gold Diaz D, Tsogbayar T, Scambler PJ, Ivins S. Loss of CXCL12/CXCR4 signalling impacts several aspects of cardiovascular development but does not exacerbate Tbx1 haploinsufficiency. *PLoS One* 2018; **13**:e0207251.
11. Hopman RK, DiPersio JF. Advances in stem cell mobilization. *Blood Rev* 2014; **28**:31–40.
12. Singh P, Mohammad KS, Pelus LM. CXCR4 expression in the bone marrow microenvironment is required for hematopoietic stem and

progenitor cell maintenance and early hematopoietic regeneration after myeloablation. *Stem Cells* 2020; **38**:849–859.
13. Ashley RL, Antoniazzi AQ, Anthony RV, Hansen TR. The chemokine receptor CXCR4 and its ligand CXCL12 are activated during implantation and placentation in sheep. *Reprod Biol Endocrinol* 2011; **9**:148.
14. Han J, Jeong W, Gu MJ, Yoo I, Yun CH, Kim J, Ka H. Cysteine-X-cysteine motif chemokine ligand 12 and its receptor CXCR4: expression, regulation, and possible function at the maternal-conceptus interface during early pregnancy in pigs. *Biol Reprod* 2018; **99**:1137–1148.
15. Wang X, Mamillapalli R, Mutlu L, Du H, Taylor HS. Chemoattraction of bone marrow-derived stem cells towards human endometrial stromal cells is mediated by estradiol regulated CXCL12 and CXCR4 expression. *Stem Cell Res* 2015; **15**:14–22.
16. Sharma M, Afrin F, Satija N, Tripathi RP, Gangenahalli GU. Stromal-derived factor-1/CXCR4 signaling: indispensable role in homing and engraftment of hematopoietic stem cells in bone marrow. *Stem Cells Dev* 2011; **20**:933–946.
17. Tsutsumi A, Okada H, Nakamoto T, Okamoto R, Yasuda K, Kanzaki H. Estrogen induces stromal cell-derived factor 1 (SDF-1/CXCL12) production in human endometrial stromal cells: a possible role of endometrial epithelial cell growth. *Fertil Steril* 2011; **95**:444–447.
18. Hanna J, Wald O, Goldman-Wohl D, Prus D, Markel G, Gazit R, Katz G, Haimov-Kochman R, Fujii N, Yagel S *et al.* CXCL12 expression by invasive trophoblasts induces the specific migration of CD16- human natural killer cells. *Blood* 2003; **102**:1569–1577.
19. Wu X, Jin LP, Yuan MM, Zhu Y, Wang MY, Li DJ. Human first-trimester trophoblast cells recruit CD56brightCD16- NK cells into decidua by way of expressing and secreting of CXCL12/stromal cell-derived factor 1. *J Immunol* 2005; **175**:61–68.
20. Lin Y, Xu L, Jin H, Zhong Y, Di J, Lin QD. CXCL12 enhances exogenous CD4+CD25+ T cell migration and prevents embryo loss in non-obese diabetic mice. *Fertil Steril* 2009; **91**:2687–2696.
21. Moridi I, Mamillapalli R, Kodaman PH, Habata S, Dang T, Taylor HS. CXCL12 attracts bone marrow-derived cells to uterine leiomyomas. *Reprod Sci* 2020; **27**:1724–1730.
22. Tal R, Liu Y, Pluchino N, Shaikh S, Mamillapalli R, Taylor HS. A murine 5-fluorouracil-based submyeloablation model for the study of bone marrow-derived cell trafficking in reproduction. *Endocrinology* 2016; **157**:3749–3759.
23. Tal R, Shaikh S, Pallavi P, Tal A, Lopez-Giraldez F, Lyu F, Fang YY, Chinchanikar S, Liu Y, Kliman HJ *et al.* Adult bone marrow progenitors become decidual cells and contribute to embryo implantation and pregnancy. *PLoS Biol* 2019; **17**:e3000421.
24. Tal R, Dong D, Shaikh S, Mamillapalli R, Taylor HS. Bone-marrow-derived endothelial progenitor cells contribute to vasculogenesis of pregnant mouse uterus dagger. *Biol Reprod* 2019; **100**:1228–1237.
25. Tal R, Kisa J, Abuwala N, Kliman HJ, Shaikh S, Chen AY, Lyu F, Taylor HS. Bone marrow-derived progenitor cells contribute to remodeling of the postpartum uterus. *Stem Cells* 2021; **39**:1489–1505.
26. Modder UI, Sanyal A, Kearns AE, Sibonga JD, Nishihara E, Xu J, O'Malley BW, Ritman EL, Riggs BL, Spelsberg TC, Khosla S. Effects of loss of steroid receptor coactivator-1 on the skeletal response to estrogen in mice. *Endocrinology* 2004; **145**:913–921.
27. Moverare S, Venken K, Eriksson AL, Andersson N, Skrtic S, Wergedal J, Mohan S, Salmon P, Bouillon R, Gustafsson JA *et al.* Differential effects on bone of estrogen receptor alpha and androgen receptor activation in orchidectomized adult male mice. *Proc Natl Acad Sci U S A* 2003; **100**:13573–13578.
28. Agarwal U, Ghalayini W, Dong F, Weber K, Zou YR, Rabbany SY, Rafii S, Penn MS. Role of cardiac myocyte CXCR4 expression in development and left ventricular remodeling after acute myocardial infarction. *Circ Res* 2010; **107**:667–676.
29. Tachibana K, Hirota S, Iizasa H, Yoshida H, Kawabata K, Kataoka Y, Kitamura Y, Matsushima K, Yoshida N, Nishikawa S *et al.* The chemokine receptor CXCR4 is essential for vascularization of the gastrointestinal tract. *Nature* 1998; **393**:591–594.
30. Zou YR, Kottmann AH, Kuroda M, Taniuchi I, Littman DR. Function of the chemokine receptor CXCR4 in haematopoiesis and in cerebellar development. *Nature* 1998; **393**:595–599.
31. Rux DR, Song JY, Swinehart IT, Pineault KM, Schlientz AJ, Trulik KG, Goldstein SA, Kozloff KM, Lucas D, Wellik DM. Regionally restricted Hox function in adult bone marrow multipotent mesenchymal stem/stromal cells. *Dev Cell* 2016; **39**:653–666.
32. Yadi H, Burke S, Madeja Z, Hemberger M, Moffett A, Colucci F. Unique receptor repertoire in mouse uterine NK cells. *J Immunol* 2008; **181**:6140–6147.
33. Zhang JH, Yamada AT, Croy BA. DBA-lectin reactivity defines natural killer cells that have homed to mouse decidua. *Placenta* 2009; **30**:968–973.
34. Taylor HS. Endometrial cells derived from donor stem cells in bone marrow transplant recipients. *JAMA* 2004; **292**:81–85.
35. Mints M, Jansson M, Sadeghi B, Westgren M, Uzunel M, Hassan M, Palmblad J. Endometrial endothelial cells are derived from donor stem cells in a bone marrow transplant recipient. *Hum Reprod* 2008; **23**:139–143.
36. Ikoma T, Kyo S, Maida Y, Ozaki S, Takakura M, Nakao S, Inoue M. Bone marrow-derived cells from male donors can compose endometrial glands in female transplant recipients. *Am J Obstet Gynecol* 2009; **201**:e601–e608.
37. Du H, Taylor HS. Contribution of bone marrow-derived stem cells to endometrium and endometriosis. *Stem Cells* 2007; **25**:2082–2086.
38. Bratincsák A, Brownstein MJ, Cassiani-Ingoni R, Pastorino S, Szalayova I, Tóth ZE, Key S, Németh K, Pickel J, Mezey E. CD45-positive blood cells give rise to uterine epithelial cells in mice. *Stem Cells* 2007; **25**:2820–2826.
39. Du H, Naqvi H, Taylor HS. Ischemia/reperfusion injury promotes and granulocyte-colony stimulating factor inhibits migration of bone marrow-derived stem cells to endometrium. *Stem Cells Dev* 2012; **21**:3324–3331.
40. Morelli SS, Rameshwar P, Goldsmith LT. Experimental evidence for bone marrow as a source of nonhematopoietic endometrial stromal and epithelial compartment cells in a murine model. *Biol Reprod* 2013; **89**:7.
41. Abuwala N, Tal R. Endometrial stem cells: origin, biological function, and therapeutic applications for reproductive disorders. *Curr Opin Obstet Gynecol* 2021; **33**:232–240.
42. Aiuti A, Webb IJ, Bleul C, Springer T, Gutierrez-Ramos JC. The chemokine SDF-1 is a chemoattractant for human CD34+ hematopoietic progenitor cells and provides a new mechanism to explain the mobilization of CD34+ progenitors to peripheral blood. *J Exp Med* 1997; **185**:111–120.
43. Abbott JD, Huang Y, Liu D, Hickey R, Krause DS, Giordano FJ. Stromal cell-derived factor-1alpha plays a critical role in stem cell recruitment to the heart after myocardial infarction but is not sufficient to induce homing in the absence of injury. *Circulation* 2004; **110**:3300–3305.
44. Hill WD, Hess DC, Martin-Studdard A, Carothers JJ, Zheng J, Hale D, Maeda M, Fagan SC, Carroll JE, Conway SJ. SDF-1 (CXCL12) is upregulated in the ischemic penumbra following stroke: association with bone marrow cell homing to injury. *J Neuropathol Exp Neurol* 2004; **63**:84–96.
45. Unzek S, Zhang M, Mal N, Mills WR, Laurita KR, Penn MS. SDF-1 recruits cardiac stem cell-like cells that depolarize in vivo. *Cell Transplant* 2007; **16**:879–886.
46. Wang Y, Deng Y, Zhou GQ. SDF-1alpha/CXCR4-mediated migration of systemically transplanted bone marrow stromal cells towards ischemic brain lesion in a rat model. *Brain Res* 2008; **1195**:104–112.
47. Yu J, Li M, Qu Z, Yan D, Li D, Ruan Q. SDF-1/CXCR4-mediated migration of transplanted bone marrow stromal cells toward areas of heart myocardial infarction through activation of PI3K/Akt. *J Cardiovasc Pharmacol* 2010; **55**:496–505.

48. Liu N, Tian J, Cheng J, Zhang J. Migration of CXCR4 gene-modified bone marrow-derived mesenchymal stem cells to the acute injured kidney. *J Cell Biochem* 2013; **114**:2677–2689.
49. Chen P, Mamillapalli R, Habata S, Taylor HS. Endometriosis stromal cells induce bone marrow mesenchymal stem cell differentiation and PD-1 expression through paracrine signaling. *Mol Cell Biochem* 2021; **476**:1717–1727.
50. Sahin Ersoy G, Zolbin MM, Cosar E, Moridi I, Mamillapalli R, Taylor HS. CXCL12 promotes stem cell recruitment and uterine repair after injury in Asherman's syndrome. *Mol Ther Methods Clin Dev* 2017; **4**:169–177.
51. Shahnazari M, Chu V, Wronski TJ, Nissenson RA, Halloran BP. CXCL12/CXCR4 signaling in the osteoblast regulates the mesenchymal stem cell and osteoclast lineage populations. *FASEB J* 2013; **27**:3505–3513.
52. Karpova D, Ritchey JK, Holt MS, Abou-Ezzi G, Monlish D, Batoon L, Millard S, Spohn G, Wiercinska E, Chendamarai E *et al.* Continuous blockade of CXCR4 results in dramatic mobilization and expansion of hematopoietic stem and progenitor cells. *Blood* 2017; **129**:2939–2949.
53. Kawabata K, Ujikawa M, Egawa T, Kawamoto H, Tachibana K, Iizasa H, Katsura Y, Kishimoto T, Nagasawa T. A cell-autonomous requirement for CXCR4 in long-term lymphoid and myeloid reconstitution. *Proc Natl Acad Sci U S A* 1999; **96**:5663–5667.
54. Ma Q, Jones D, Springer TA. The chemokine receptor CXCR4 is required for the retention of B lineage and granulocytic precursors within the bone marrow microenvironment. *Immunity* 1999; **10**: 463–471.
55. Noda M, Omatsu Y, Sugiyama T, Oishi S, Fujii N, Nagasawa T. CXCL12-CXCR4 chemokine signaling is essential for NK-cell development in adult mice. *Blood* 2011; **117**:451–458.
56. Brighton PJ, Maruyama Y, Fishwick K, Vrljicak P, Tewary S, Fujihara R, Muter J, Lucas ES, Yamada T, Woods L *et al.* Clearance of senescent decidual cells by uterine natural killer cells in cycling human endometrium. *Elife* 2017; **6**:e31274.
57. Lucas ES, Dyer NP, Murakami K, Lee YH, Chan YW, Grimaldi G, Muter J, Brighton PJ, Moore JD, Patel G *et al.* Loss of endometrial plasticity in recurrent pregnancy loss. *Stem Cells* 2016; **34**: 346–356.
58. Lucas ES, Vrljicak P, Muter J, Diniz-da-Costa MM, Brighton PJ, Kong CS, Lipecki J, Fishwick KJ, Odendaal J, Ewington LJ *et al.* Recurrent pregnancy loss is associated with a pro-senescent decidual response during the peri-implantation window. *Commun Biol* 2020; **3**:37.
59. Diniz-da-Costa M, Kong CS, Fishwick KJ, Rawlings T, Brighton PJ, Hawkes A, Odendaal J, Quenby S, Ott S, Lucas ES *et al.* Characterization of highly proliferative decidual precursor cells during the window of implantation in human endometrium. *Stem Cells* 2021; **39**:1067–1080.
60. Dominguez F, Galan A, Martin JJ, Remohi J, Pellicer A, Simon C. Hormonal and embryonic regulation of chemokine receptors CXCR1, CXCR4, CCR5 and CCR2B in the human endometrium and the human blastocyst. *Mol Hum Reprod* 2003; **9**:189–198.
61. Vento-Tormo R, Efremova M, Botting RA, Turco MY, Vento-Tormo M, Meyer KB, Park JE, Stephenson E, Polanski K, Goncalves A *et al.* Single-cell reconstruction of the early maternal-fetal interface in humans. *Nature* 2018; **563**:347–353.
62. Garcia-Alonso L, Handfield LF, Roberts K, Nikolakopoulou K, Fernando RC, Gardner L, Woodhams B, Arutyunyan A, Polanski K, Hoo R *et al.* Mapping the temporal and spatial dynamics of the human endometrium in vivo and in vitro. *Nat Genet* 2021; **53**: 1698–1711.
63. Kouzeli A, Collins PJ, Metzemaekers M, Meyrath M, Szpakowska M, Artinger M, Struyf S, Proost P, Chevigne A, Legler DF *et al.* CXCL14 preferentially synergizes with homeostatic chemokine receptor systems. *Front Immunol* 2020; **11**:561404.
64. Collins PJ, McCully ML, Martinez-Munoz L, Santiago C, Wheeldon J, Caucheteux S, Thelen S, Cecchinato V, Laufer JM, Purvanov V *et al.* Epithelial chemokine CXCL14 synergizes with CXCL12 via allosteric modulation of CXCR4. *FASEB J* 2017; **31**:3084–3097.
65. Wu X, Li DJ, Yuan MM, Zhu Y, Wang MY. The expression of CXCR4/CXCL12 in first-trimester human trophoblast cells. *Biol Reprod* 2004; **70**:1877–1885.
66. Zhou WH, Du MR, Dong L, Yu J, Li DJ. Chemokine CXCL12 promotes the cross-talk between trophoblasts and decidual stromal cells in human first-trimester pregnancy. *Hum Reprod* 2008; **23**: 2669–2679.
67. Staun-Ram E, Goldman S, Gabarin D, Shalev E. Expression and importance of matrix metalloproteinase 2 and 9 (MMP-2 and -9) in human trophoblast invasion. *Reprod Biol Endocrinol* 2004; **2**:59.
68. Koo HS, Yoon MJ, Hong SH, Ahn J, Cha H, Lee D, Ko JE, Kwon H, Choi DH, Lee KA *et al.* CXCL12 enhances pregnancy outcome via improvement of endometrial receptivity in mice. *Sci Rep* 2021; **11**:7397.
69. Tewary S, Lucas ES, Fujihara R, Kimani PK, Polanco A, Brighton PJ, Muter J, Fishwick KJ, Da Costa M, Ewington LJ *et al.* Impact of sitagliptin on endometrial mesenchymal stem-like progenitor cells: a randomised, double-blind placebo-controlled feasibility trial. *EBioMedicine* 2020; **51**:102597.
70. Suzuki Y, Rahman M, Mitsuya H. Diverse transcriptional response of CD4+ T cells to stromal cell-derived factor SDF-1: cell survival promotion and priming effects of SDF-1 on CD4+ T cells. *J Immunol* 2001; **167**:3064–3073.